



HAL
open science

Uniaxial deformation tests of aqueous foams: rate effects and topological changes

M Emilia Rosa, Manuel Fortes

► **To cite this version:**

M Emilia Rosa, Manuel Fortes. Uniaxial deformation tests of aqueous foams: rate effects and topological changes. *Philosophical Magazine*, 2006, 86 (32), pp.4997-5007. 10.1080/14786430600743868 . hal-00513704

HAL Id: hal-00513704

<https://hal.science/hal-00513704>

Submitted on 1 Sep 2010

HAL is a multi-disciplinary open access archive for the deposit and dissemination of scientific research documents, whether they are published or not. The documents may come from teaching and research institutions in France or abroad, or from public or private research centers.

L'archive ouverte pluridisciplinaire **HAL**, est destinée au dépôt et à la diffusion de documents scientifiques de niveau recherche, publiés ou non, émanant des établissements d'enseignement et de recherche français ou étrangers, des laboratoires publics ou privés.



Uniaxial deformation tests of aqueous foams: rate effects and topological changes

Journal:	<i>Philosophical Magazine & Philosophical Magazine Letters</i>
Manuscript ID:	TPHM-05-Aug-0374.R2
Journal Selection:	Philosophical Magazine
Date Submitted by the Author:	06-Apr-2006
Complete List of Authors:	Rosa, M Emilia; ICEMS - IST, Engenharia de Materiais Fortes, Manuel; Instituto Superior Tecnico, Departamento de Engenharia de Materiais
Keywords:	bubbles, foams
Keywords (user supplied):	aerosols and foams, heterogeneous liquids



Uniaxial deformation tests of aqueous foams: rate effects and topological changes

M. EMÍLIA ROSA* and M. A. FORTES

ICEMS-Instituto de Ciência e Engenharia de Materiais e Superfícies
Departamento de Engenharia de Materiais, Instituto Superior Técnico
Av. Rovisco Pais, 1049-001 Lisboa, Portugal

* M. Emília Rosa

Telephone: 351 21 8418105

Fax: 351 21 8418132

E-mail address: emilia.rosa@ist.utl.pt

M. A. Fortes

Telephone: 351 21 8418118

Fax: 351 21 8418132

E-mail address: l.marcelino@ist.utl.pt

Uniaxial deformation tests of aqueous foams: rate effects and topological changes

M. EMÍLIA ROSA* and M. A. FORTES

ICEMS-Instituto de Ciência e Engenharia de Materiais e Superfícies
Departamento de Engenharia de Materiais, Instituto Superior Técnico
Av. Rovisco Pais, 1049-001 Lisboa, Portugal

ABSTRACT

We have experimentally obtained force – elongation, $F(w)$, curves for the uniaxial extension/compression of single cylindrical bubbles and bubble clusters bounded by two horizontal walls at a variable separation w . We have studied the effect of the elongation rate on $F(w)$ of cylindrical bubbles and the changes in F associated with instabilities and with topological transformations that occur during deformation of bubble clusters.

Keywords: PACS. 82.70Rr – Aerosols and foams

PACS. 83.70Hq – Heterogeneous liquids: suspensions, dispersions, emulsions, pastes, slurries, foams, block copolymers, etc.

1. Introduction

At low enough strains liquid foams deform elastically. The liquid films stretch or contract reversibly and the size of the Plateau borders (PB) changes but the topology is preserved, *i. e.* each bubble remains surrounded by the same bubbles [1, 2]. Elastic deformation of a foam is accompanied by liquid flow in the films and Plateau borders (and also in the PB quadruple junctions) and because flow is dissipative, the term viscoelastic is more appropriate for the foam deformation regime in which no

1
2
3 topological changes occur. Thus there are strain rate effects in foam deformation. One
4 of the purposes of this paper is to report on experiments aimed at studying these rate
5 effects in the uniaxial deformation of a cylindrical bubble confined by two parallel
6 walls; we obtained force – displacement curves for various displacement rates.
7 Recently, considerable attention has been given to the effects of viscous drag on the
8 flow of foams [3-7]. Dissipative forces are associated with the flow of liquid in the
9 films and Plateau borders and with the drag of wall Plateau borders as they slide along
10 the confining walls as discussed in the early works of Bretherton [8], Schwartz and
11 Princen [9] and Reinelt and Kraynik [10]. Our results may provide a good test for
12 theories of foam rheology that incorporate viscous drag.
13
14
15
16
17
18
19
20

21 At higher strains topological changes occur in a foam, either locally, involving a
22 small number of bubbles, or in avalanches which affect a large number of bubbles in
23 succession [1, 11-13]. The topological changes give rise to discontinuities or jumps in
24 the applied force, the amplitude of which depends on the number of elementary T1
25 topological changes in the avalanches. We report on foam deformation experiments in
26 which we observed these features in many-bubble three-dimensional (3D) clusters.
27
28
29
30
31

32 Finally we also obtained force – displacement curves for the uniaxial
33 compression of a 3D bubble cluster consisting of two equal bubbles one on top of the
34 other (twin bubble). These exhibit a symmetry breaking transition with no change in
35 topology followed by a topological change. This cluster was studied in detail by Bohn
36 [14] and subsequently by Fortes *et al.* [15].
37
38
39
40
41
42
43

44 2. EXPERIMENTAL

45
46
47 We used a Wilhelmy balance to measure the force F required to deform 3D bubble
48 clusters bounded by two horizontal walls, the separation w of which could be varied at a
49 constant rate, $v = |\dot{w}|$. The Wilhelmy balance is commonly used for the measurement of
50 the dynamic surface tension of liquids (*e.g.* [16]).
51
52
53
54

55 The bubble systems tested were a single cylindrical bubble, a twin bubble (two
56 bubbles of the same volume, one on top of the other) and many-bubble clusters. The
57 bubbles were bounded by a perspex plate at the top, suspended from the arm of the
58 balance, and, in most cases, a liquid pool (the commercial detergent solution used in the
59
60

1
2
3
4 preparation of the bubble clusters) at the bottom. The surface tension γ_L of the bulk
5 liquid solution measured by the sessile drop method was $\gamma_L = 35.0 \text{ mN m}^{-1}$.
6
7 Experiments with a horizontal plate replacing the pool were also made for single
8 bubbles, but the stability of the bubbles was so poor that only very small variations in w
9 could be achieved. The films contact the plates and the pool at approximately 90° and
10 are free to slide on both of them.
11
12

13
14 The cylindrical bubble (Fig. 1(a)) was prepared from a hemispherical bubble
15 formed on the top plate by blowing a volume V of air with a syringe into a small drop of
16 the detergent solution sitting on the plate. The hemispherical bubble was then forced to
17 contact the liquid pool (or plate) below producing a cylindrical bubble of volume V .
18
19

20
21 The preparation of a twin bubble required a special procedure (direct preparation
22 from two bubbles did not work): three bubbles of the same volume, were blown with a
23 syringe on the top plate to form a cluster which was then forced to contact the liquid
24 pool, producing a layer with three sandwiched bubbles. By increasing the plate/pool
25 separation one of the bubbles jumped to a second layer. Finally one of the two bubbles
26 in the other layer was destroyed by means of a metal pin, thus forming the twin bubble
27 configuration of Fig. 1(b) with a horizontal inter-bubble film.
28
29

30
31 Many-bubble clusters were prepared by blowing 10 to 20 bubbles of nearly the
32 same volume, around 30 mm^3 , in a pile on the plate. The cluster was then forced to
33 contact the pool originating a multilayer cluster bounded by the pool surface and the
34 plate above (Fig. 1(c)).
35
36
37
38
39
40
41

42 43 **Insert Figure 1**

44
45
46
47 In all experiments the top plate was suspended from the arm of the balance and
48 the (vertical) force was set to zero ($F = 0$) before forming the bubble cluster. The
49 separation w was then increased or decreased at a constant rate $v = |\dot{w}|$ thus causing
50 uniaxial deformation of the cluster. The velocities available were (in mm min^{-1}): 1, 5,
51 10, 20 and 30. The applied force F was recorded every second (for any velocity), from
52 which $F(w)$ was derived. All data refers to a bubble or cluster bounded by a liquid pool
53 at the bottom.
54
55
56
57
58
59
60

3. RESULTS AND DISCUSSION

3.1. Single cylindrical bubble

Under static conditions ($v = 0$) the force F on the plate is

$$F_0 = F(v = 0) = \pi R \gamma_0 \quad (1)$$

where R is the radius of the bubble cross-section and γ_0 is the (static) film tension, both being assumed as uniform along the bubble. The force F_0 is the sum of a force $2\pi R \gamma_0$ due to the contractile tendency of the film and an opposite force $\pi R \gamma_0$ that results from the pressure difference γ_0/R across the film, acting on the area πR^2 . Since the bubble volume $V = \pi R^2 w$, we can write equation (1) as

$$\frac{F_0}{\gamma_0 V^{1/3}} = \pi^{1/2} \left(\frac{w}{V^{1/3}} \right)^{-1/2} \quad (2)$$

This equation can also be derived from $F_0 = \frac{dE}{dw}$ where E is the bubble surface energy given by $E = 2\pi R w \gamma_0 = 2(\pi V)^{1/2} \gamma_0 w^{1/2}$. We measured the static force F_0 for bubbles of two volumes V (2 and 4 cm³) at various w for each volume. Figure 2 shows plots of $\frac{F_0}{V^{1/3}}$ as a function of $\left(\frac{w}{V^{1/3}} \right)^{-1/2}$ for the two bubble volumes. The two plots coincide and lead to $\gamma_0 = 73.1 \text{ mN m}^{-1}$. This is, as expected, about twice the bulk liquid surface tension γ_L .

Insert Figure 2

Figures 3(a) and 3(b) show experimental force – displacement, or $F(w)$ curves for cylindrical bubbles of volumes $V = 2 \text{ cm}^3$ and $V = 4 \text{ cm}^3$ deformed at three of the

1
2
3 five deformation rates ν available. The curves were obtained with different bubbles of
4 the same volume. The curves of Figs. 3(a) and 3(b) are drawn by connecting the (F, w)
5 points read off the balance. The force F is always tensile and decreases with increasing
6 w . At fixed w , the force increases with increasing deformation rate ν , both in elongation
7 and in compression, the force increment for a given change in ν being nearly
8 independent of w .
9

10 We found that the $F(w)$ curves in elongation-compression coincide. The sliding
11 velocity $v_{\text{slid}} = \left| \frac{dR}{dt} \right|$ of the Plateau borders and liquid meniscus relates to the
12 deformation velocity $\nu = \left| \frac{dw}{dt} \right|$ by
13

$$v_{\text{slid}} = \left(\frac{V}{4\pi w^3} \right)^{1/2} \nu \quad (3)$$

14 since $V = \pi R^2 w$ is constant. For the same V , ν and w the absolute value of the sliding
15 velocity is the same. Thus, we expect reversibility of the $F(w)$ curve for a given ν . It
16 should be noted that irreversibility in foam deformation is due to topological neighbour
17 switching events as in the work of Jiang *et al.* [12] on 2D foams. These events are
18 absent in the deformation of a single bubble.
19

20 Insert Figure 3

21 When the liquid pool at the bottom was replaced by a perspex plate, the
22 measured force for the same V , w and ν , was slightly larger *i. e.*, drag forces are larger
23 with a liquid pool. This is probably due to the replacement of a Plateau border at the
24 bottom by a liquid meniscus, which increases the film thickness and the size of the
25 Plateau border at the plate. **Note that for $\nu = 0$ the (static) force is the same for the plate-
26 pool and plate-plate boundaries.**

27 We also carried out tests in which the deformation rate ν was suddenly changed
28 during deformation of a cylindrical bubble. Examples of the resulting $F(w)$ curves are
29 in Fig. 3(c) for rate reductions from $\nu = 30$ and 10 mm min^{-1} to $\nu = 1 \text{ mm min}^{-1}$ in the
30

1
2
3 elongation of a bubble with $V = 2 \text{ cm}^3$. A transient is observed following the velocity
4 change, analogous to the transient at the onset of deformation (change from $v = 0$ to a
5 non-zero v) which can be detected in the curves of Figs. 3(a) and (b).
6
7

8
9 In Figs. 4(a) and 4(b) we show the experimental data (excluding the transient in
10 force) obtained for bubbles of $V = 2 \text{ cm}^3$ and $V = 4 \text{ cm}^3$, respectively, deformed at
11 various elongation rates, in the form of a plot of $\frac{F}{\pi R \gamma_0} = \frac{F}{F_0}$ as a function of $\frac{w}{V^{1/3}}$.
12
13

14
15
16 The radius R is obtained from $V = \pi R^2 w$. The horizontal segments on the left of Figs.
17 4(a) and 4(b) are for the average $\frac{F}{\pi R \gamma_0}$ for each elongation rate. We used these
18
19 average values to determine the exponent n in the relation between the excess force per
20 unit circumferential length and the elongation velocity
21
22
23
24
25
26
27

$$\frac{F - F_0}{2\pi R \gamma_0} = \left(\frac{v}{v^*} \right)^n \quad (4)$$

28
29
30
31
32
33 where v^* is a constant velocity. The log – log plots of Fig. 4(c) give for the best fit
34 exponent $n = 1.02$ for both volumes (straight lines in Fig. 4(c)) and the constant
35
36
37 $v^* = 36.3 \text{ mm s}^{-1}$ for $V = 2 \text{ cm}^3$ and $v^* = 22.2 \text{ m s}^{-1}$ for $V = 4 \text{ cm}^3$.
38
39
40

41 **Insert Figure 4**

42
43
44 Bretherton [8] predicted a power law relation with exponent $n = 2/3$ between
45 the sliding friction force F_{slid} per unit length of a PB and the sliding velocity v_{slid} (both
46 parallel to the plate): $F_{\text{slid}} \propto v_{\text{slid}}^n$. This is close to the exponent n obtained in
47 experiments by Cantat *et al.* [3] on foam sliding on a plate. In our experiments sliding is
48 induced by a vertical excess force $(F - F_0)$ and the velocity v is vertical. The sliding
49 velocity v_{slid} relates to v by equation (3), but the relation between F_{slid} and the excess
50 force $(F - F_0)/2\pi R$ is not known. Besides, the mechanism of dissipation in our
51 experiments is not exclusively sliding of the PB at the top plate. It is therefore not
52
53
54
55
56
57
58
59
60

surprising that we obtain an exponent $n \cong 1$ in equation (4), which deviates from that predicted by Bretherton [8].

3.2. Twin bubble

At large separations, w , of the confining walls the inter-bubble circular film in a twin bubble is horizontal (Fig. 1(b)) and joins the curved films at 120° under equilibrium. As w decreases to a critical w_0^* for which $F = 0$, a buckling instability arises at which the inter-bubble film starts tilting; its tilt relative to the confining walls increases as w is further decreased until at w_1^* the inter-bubble film touches the confining walls and a topological transition occurs whereby the film further rotates to a configuration with two vertical cylindrical bubbles contacting at a vertical planar film (see Fig. 1(b)) which we term the vertical twin bubble. This buckling instability, under static conditions, was analysed in detail by Bohn [14], who found $w_0^* = 0.886V^{1/3}$ and $w_1^* = 0.767V^{1/3}$ for a twin bubble with V the volume of each bubble. Bohn also found that during the (static) buckling transition, *i.e.* for w between w_0^* and w_1^* , the force $F = 0$. For $w < w_1^*$, the vertical twin bubble forms and the force under static conditions is given by

$$F = \lambda V^{1/2} \gamma_0 w^{-1/2} \quad \lambda = \left(\frac{8\pi}{3} + \sqrt{3} \right)^{1/2} \cong 3.1796 \quad (5)$$

which can be derived along the same lines as equation (2), noting that the radius of the curved films, R' , relates to the cross-sectional area A of each bubble by $R' = \frac{2}{\lambda} A^{1/2}$ (angles of 120° at film junctions).

In Fig. 5 we show an experimental force – displacement curve for a twin bubble ($V = 1\text{cm}^3$) compressed at 5mm min^{-1} . The $F(w)$ plot has two main branches (full lines): the small F (large w) branch refers to the twin bubble, while the large F (small w) branch refers to the vertical twin bubble. For the twin bubble $dF/dw > 0$ and the force reaches $F = 0$ at $w_0^* \cong 0.8V^{1/3}$ (Fig. 5) in good agreement with the value predicted by Bohn [14] for the static twin bubble referred to above. While the planar inter-bubble film rotates to reach the confining horizontal walls, the force remains at zero (Fig. 1(b))

1
2
3 and w changes from w_0^* to w_1^* . On further decreasing w , the force rises from zero to
4
5 2.6 mN (dashed line in Fig. 5) and the vertical twin bubble forms (Fig. 1(b)). The
6
7 duration of this topological transition is about 6 s. The force F on the confining walls,
8
9 under static conditions is given by equation (5). For $w = w_1^*$, equation (5) gives F close
10
11 to the experimental value 2.6 mN. Following this jump, the force increases with
12
13 decreasing w (in the low w branch). We found that $F \propto w^{-1/2}$ in this branch, as for
14
15 static deformation (equation (5)).
16
17

18
19 **Insert Figure 5**
20
21

22 23 3.3. Many-bubble cluster 24 25

26
27 Figure 6 shows force – time data points for a fairly monodisperse 3D cluster with 10
28
29 bubbles (bubble volume V around 30 mm^3), confined by a plate and a pool surface,
30
31 deformed in successive elongation – compression cycles, with the applied force F
32
33 varying over a 4 mN range. The displacement rate in this test was $v = 5 \text{ mm min}^{-1}$.
34
35 Similar curves were obtained with other many-bubble clusters but we did not study the
36
37 effect of v . The $dF/dt > 0$ regions of the curve correspond to compression ($\dot{w} < 0$) and
38
39 those with $dF/dt < 0$ to elongation ($\dot{w} > 0$). The curve of Fig. 6 resembles those
40
41 obtained in simulations of two-dimensional bubble clusters in [1].
42
43

44
45 **Insert Figure 6**
46
47

48
49 The force – time $F(t)$ data of Fig. 6 show sudden force changes ΔF associated
50
51 with topological transitions. These occur when there is a decrease (in compression) or
52
53 increase (in elongation) in the number of layers in the cluster (from 1 to 3 layers) due to
54
55 bubble rearrangements (isolated or in avalanches). Between the jumps the foam deforms
56
57 elastically. For example, at large F (typically small w) there are relatively large intervals
58
59 of w with no jumps in F , which are associated with pure elastic deformation of the one-
60
cylindrical bubble. The average slope $|dF/dw|$ of these regions is around

0.9 mN mm⁻¹. It is worth noting that under extension the bubble monolayer survives past the force (at A in Fig. 6) where it first appears in compression (at A'). The fact that the first peak in F occurs at larger F than the other two, is probably due to bursting of a few bubbles at the cluster free surface.

The discontinuities in F at lower F 's are due to neighbour switching topological changes, which alter the number of bubble layers and the number of bubbles in each layer. Most values of ΔF associated with topological changes are around 0.1 mN ($\Delta F/\gamma_0 V^{1/3} \cong 0.5$), but a few are much larger (up to 0.9 mN), probably associated with avalanches of topological transitions. The number of topological transitions when w changes by $\Delta w = 8.3$ mm ($\Delta t \cong 100$ s) is between 3 and 6. The variation of w per topological change is thus 1.4 – 2.8 mm, close to the average bubble diameter.

4. SUMMARY

We have reported on experiments conducted with a Wilhelmy balance aimed at obtaining force – displacement $F(w)$ curves of foams under uniaxial deformation. We studied the effect of the deformation rate on the $F(w)$ curves for a single cylindrical bubble and attempted to fit the data to a power law relating force and deformation rate. We have also studied the effect on $F(w)$ of topological transitions and symmetry breaking instabilities that occur during the deformation of foam clusters. These lead to discontinuities in the force F or in dF/dw , separating regions of continuous elastic deformation.

Acknowledgements

We thank L. Afonso for his help with the experiments, and D. Weaire and P. I. C. Teixeira for their comments on the manuscript.

References

- [1] D. Weaire and S. Hutzler, *The Physics of Foams* (Oxford University Press, Oxford, 1999).
- [2] D. Weaire and M. A. Fortes, *Advances in Physics*, **43** 685 (1994).
- [3] I. Cantat, N. Kern and R. Delannay, *Europhysics Letters*, **65** 726 (2004).
- [4] S. Cohen-Addad, R. Höhler and Y. Khidas, *Physical Review Letters*, **93** 028302 (2004).
- [5] N. Kern, D. Weaire, A. Martin, S. Hutzler and S. J. Cox, *Physical Review E*, **70** 041411 (2004).
- [6] S. J. Cox, *Colloids and Surface A: Physicochem Eng. Aspects*, **263** 81 (2005).
- [7] N. D. Denkov, V. Subramanian, D. Gurovich and A. Lips, *Colloids and Surface A: Physicochem Eng. Aspects*, **263** 129 (2005).
- [8] F. J. Bretherton, *Journal of Fluid Mechanics*, **10** 166 (1961).
- [9] L. W. Schwartz and H. M. Princen, *Journal of Colloid and Interface Science*, **118** 201 (1987).
- [10] D. A. Reinelt and A. M. Kraynik, *Journal of Colloid and Interface Science*, **132** 491 (1989).
- [11] M. E. Rosa and M. A. Fortes, *Philosophical Magazine A*, **77** 1423 (1998).
- [12] Y. Jiang, P. J. Swart, A. Saxena, M. Asipauskas and J. A. Glazier, *Physical Review E*, **59** 5819 (1999).
- [13] M. E. Rosa, M. A. Fortes and M. F. Vaz, *The European Physical Journal E*, **7** 129

1
2
3 (2002).
4
5
6

7 [14] S. Bohn, *The European Physical Journal*, **11** 177 (2003).
8
9

10 [15] M. A. Fortes, M. E. Rosa, M. F. Vaz and P. I. C. Teixeira, *The European Physical*
11 *Journal E*, **15** 395 (2004).
12
13

14
15 [16] A. W. Adamson, *Physical Chemistry of Surfaces* (John Wiley & Sons, New York,
16 1990).
17
18
19
20
21
22
23
24
25
26
27
28
29
30
31
32
33
34
35
36
37
38
39
40
41
42
43
44
45
46
47
48
49
50
51
52
53
54
55
56
57
58
59
60

Figure captions

Figure 1 – Side views of: (a) Single cylindrical bubble; (b) Twin-bubble: “horizontal” (initial configuration), buckled and “vertical” configurations; (c) Many-bubble cluster with three layers of bubbles. The Plateau borders and the liquid menisci are not shown.

Figure 2 – The measured reduced static force $\frac{F_0}{V^{1/3}}$ for cylindrical bubbles of volume $V = 2 \text{ cm}^3$ (◆) and $V = 4 \text{ cm}^3$ (■) as a function of $\left(\frac{w}{V^{1/3}}\right)^{-1/2}$; w is the height of the bubble.

Figure 3 – Force (F) – bubble height (w) curves obtained in tensile tests at different elongation rates: (—) 30 mm min^{-1} , (---) 10 mm min^{-1} , and (⋯) 1 mm min^{-1} for cylindrical bubbles of volume: (a) $V = 2 \text{ cm}^3$ and (b) $V = 4 \text{ cm}^3$. (c) $F(w)$ curves with sudden deformation rate change undertaken at $w = 12 \text{ mm}$ for bubbles with $V = 2 \text{ cm}^3$; the initial rates were: (—) 30 mm min^{-1} and (---) 10 mm min^{-1} ; the final rate was 1 mm min^{-1} in both cases. In (a), (b) and (c) the curves are fits to the experimental points, which are shown (squares) only for $v = 30 \text{ mm min}^{-1}$ in (a).

Figure 4 – The reduced force $\frac{F}{\pi R \gamma_0} = \frac{F}{F_0}$ to deform a cylindrical bubble of radius R and volume $V = \pi R^2 w$, as a function of $\frac{w}{V^{1/3}}$ for the various elongation rates used: (□) 30 mm min^{-1} , (◇) 20 mm min^{-1} , (▲) 10 mm min^{-1} , (■) 5 mm min^{-1} and (◆) 1 mm min^{-1} . w is the bubble height and γ_0 is the static film tension. The horizontal segments indicate the average values for each v . Bubble volumes: (a) $V = 2 \text{ cm}^3$ and (b) $V = 4 \text{ cm}^3$. (c) Log – log plot of the

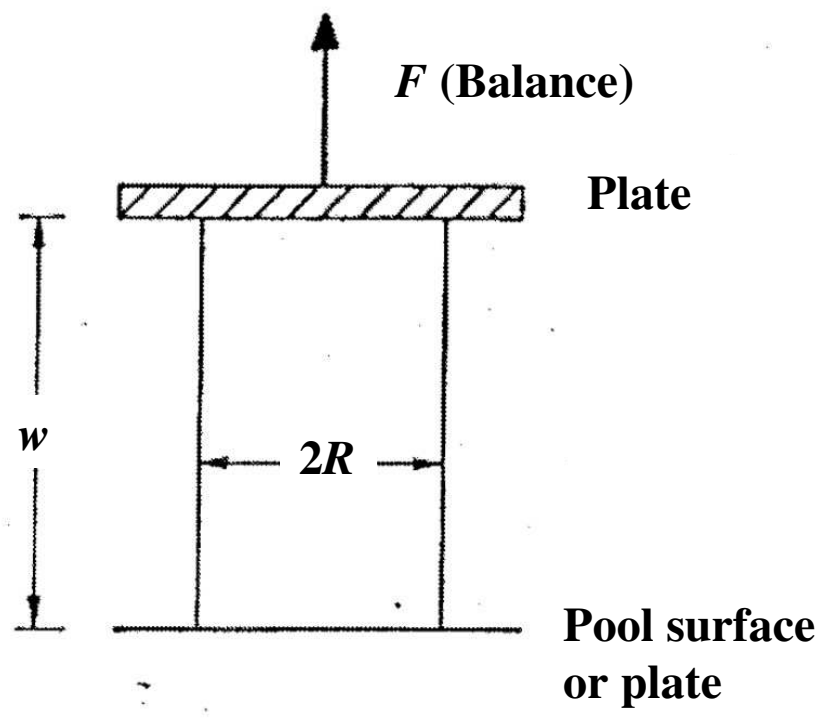
1
2
3
4 force increment $\frac{F - F_0}{2\pi R\gamma_0}$ required to deform a cylindrical bubble at an
5
6
7 elongation rate v , for the two bubble volumes: (◆) $V = 2\text{ cm}^3$ and
8
9 (■) $V = 4\text{ cm}^3$. F_0 is the static force for $v = 0$.
10
11

12
13 Figure 5 – Force (F) – cluster height (w) curve obtained in a compression test of a twin
14
15 bubble cluster ($V = 1000\text{ mm}^3$) at a compression $v = 5\text{ mm min}^{-1}$, starting at
16
17 $w = 16\text{ mm}$. Buckling occurs in the narrow interval where $F = 0$. The force
18
19 jump from $F = 0$ to $F = 2.6\text{ mN}$ (dashed line), is associated with the
20
21 topological change at the end of buckling to a vertical twin bubble (see Fig.
22
23 1(b)). Experimental points are not shown. The insert shows a zoom of the
24
25 curve region around $F = 0$.
26
27

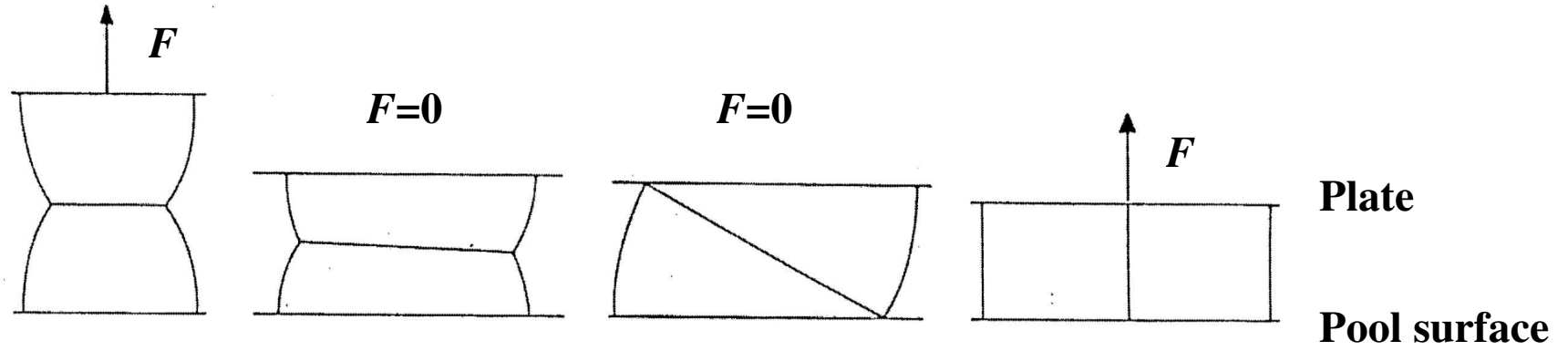
28
29 Figure 6 - Force (F) – time (t) data points obtained in extension – compression cycles of
30
31 a fairly monodisperse three-dimensional 10-bubble cluster (average bubble
32
33 volume $\cong 30\text{ mm}^3$). The top, smoother regions correspond to elastic
34
35 deformation of a single layer of bubbles. Subsequently bubbles jump to build a
36
37 second layer (starting at A) and then a third layer (at B) in extension and vice-
38
39 versa in compression.
40
41
42
43
44
45
46
47
48
49
50
51
52
53
54
55
56
57
58
59
60

1
2
3
4
5
6
7
8
9
10
11
12
13
14
15
16
17
18
19
20
21
22
23
24
25
26
27
28
29
30
31
32
33
34
35
36
37
38
39
40
41
42
43
44
45
46
47
48
49
50
51
52
53
54
55
56
57
58
59
60

EM



only



$$w > w_0^*$$

$$w_0^* > w > w_1^*$$

$$w = w_1^*$$

$$w < w_1^*$$

$$\frac{dF}{dw} > 0$$

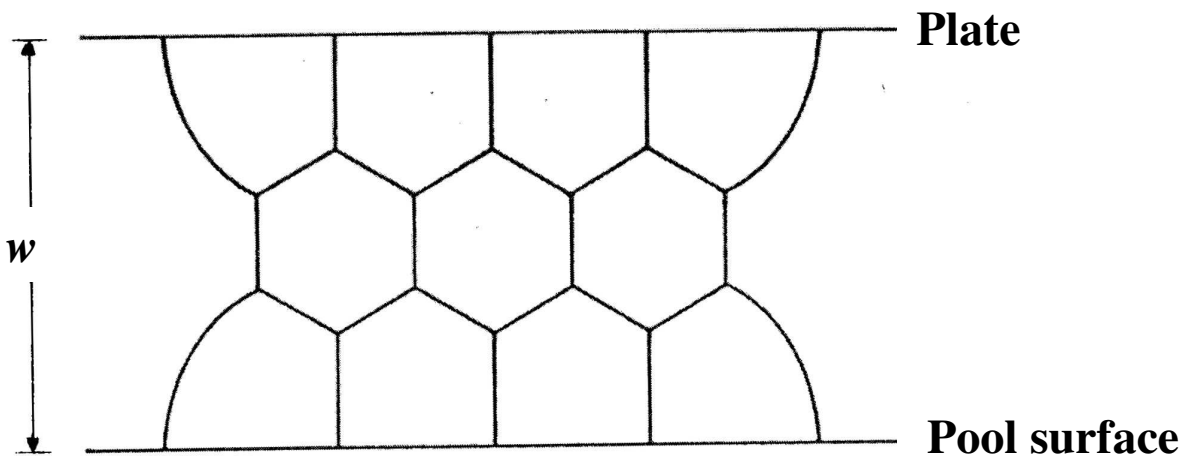
$$\frac{dF}{dw} = 0$$

$$\frac{dF}{dw} < 0$$

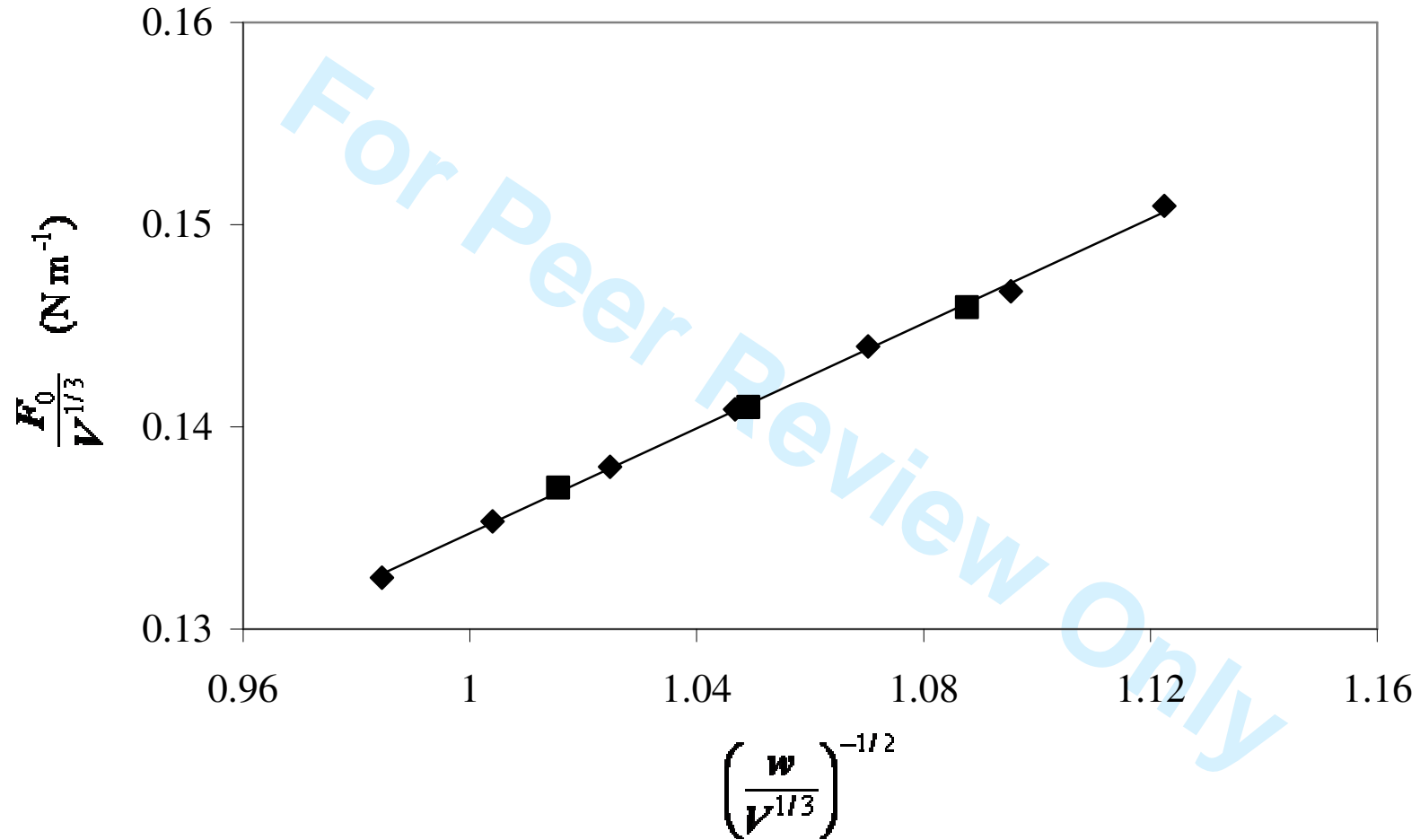


1
2
3
4
5
6
7
8
9
10
11
12
13
14
15
16
17
18
19
20
21
22
23
24
25
26
27
28
29
30
31
32
33
34
35
36
37
38
39
40
41
42
43
44
45
46
47

1
2
3
4
5
6
7
8
9
10
11
12
13
14
15
16
17
18
19
20
21
22
23
24
25
26
27
28
29
30
31
32
33
34
35
36
37
38
39
40
41
42
43
44
45
46
47
48
49
50
51
52
53
54
55
56
57
58
59
60

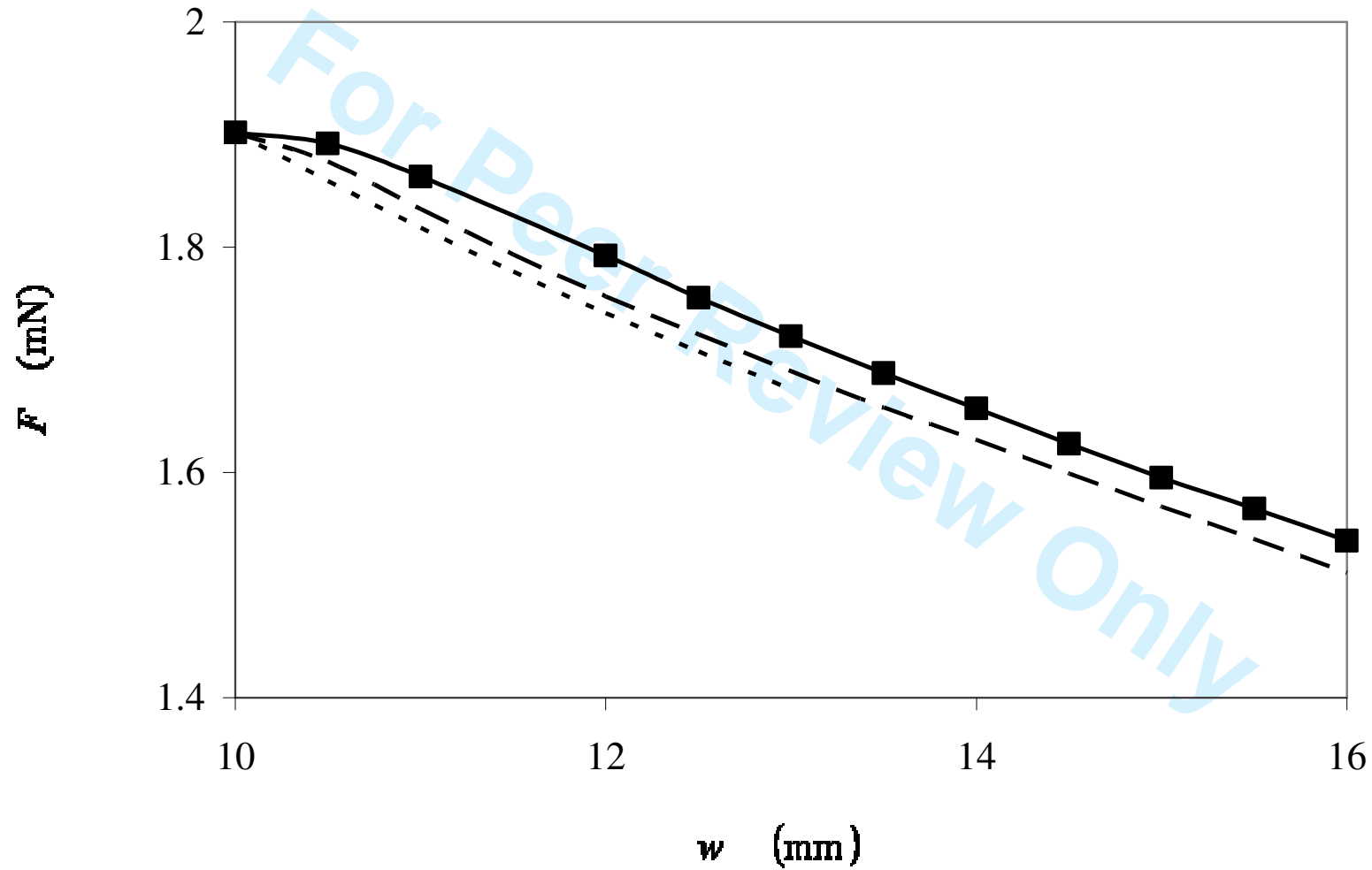


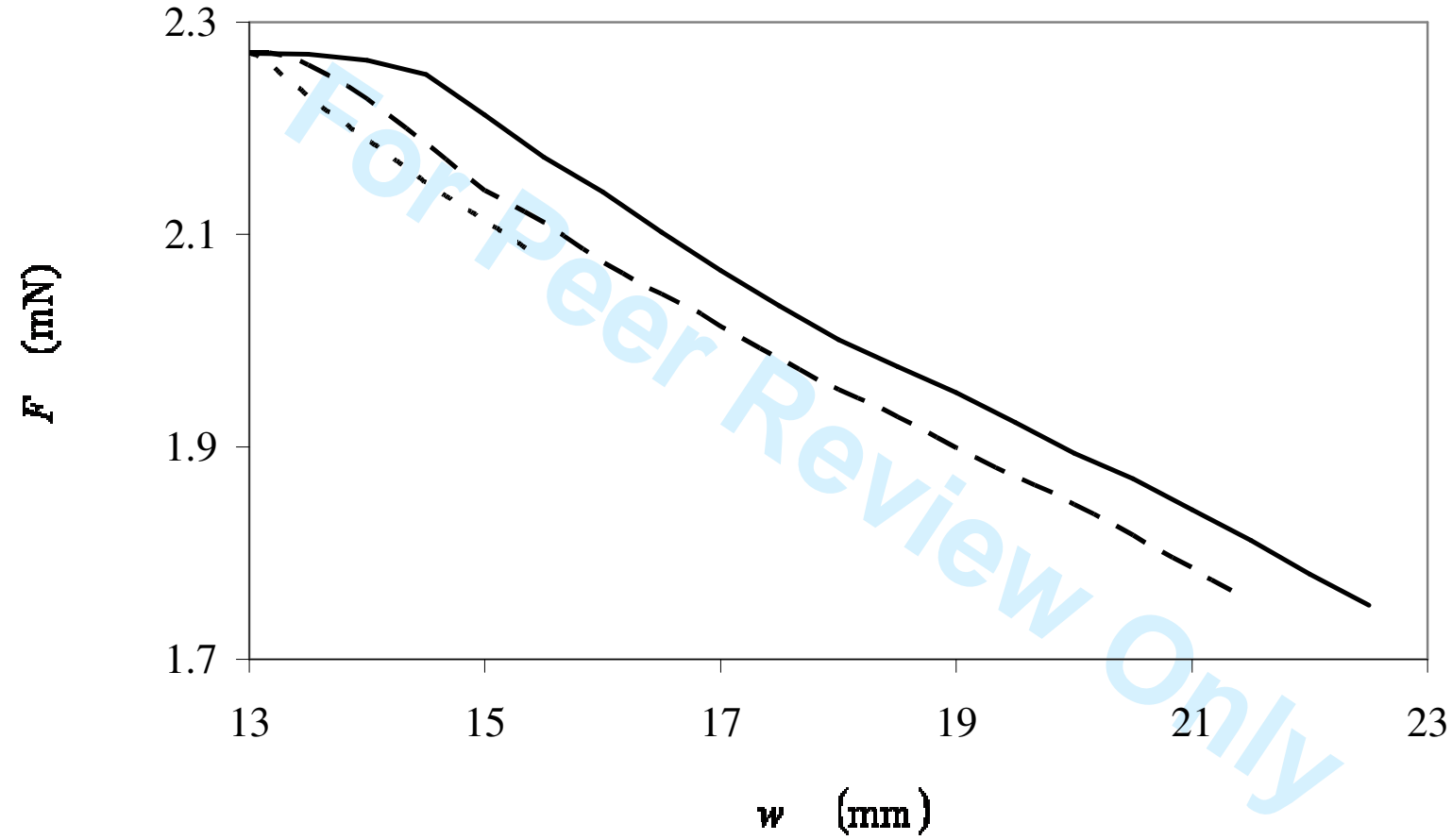
Peer Review Only



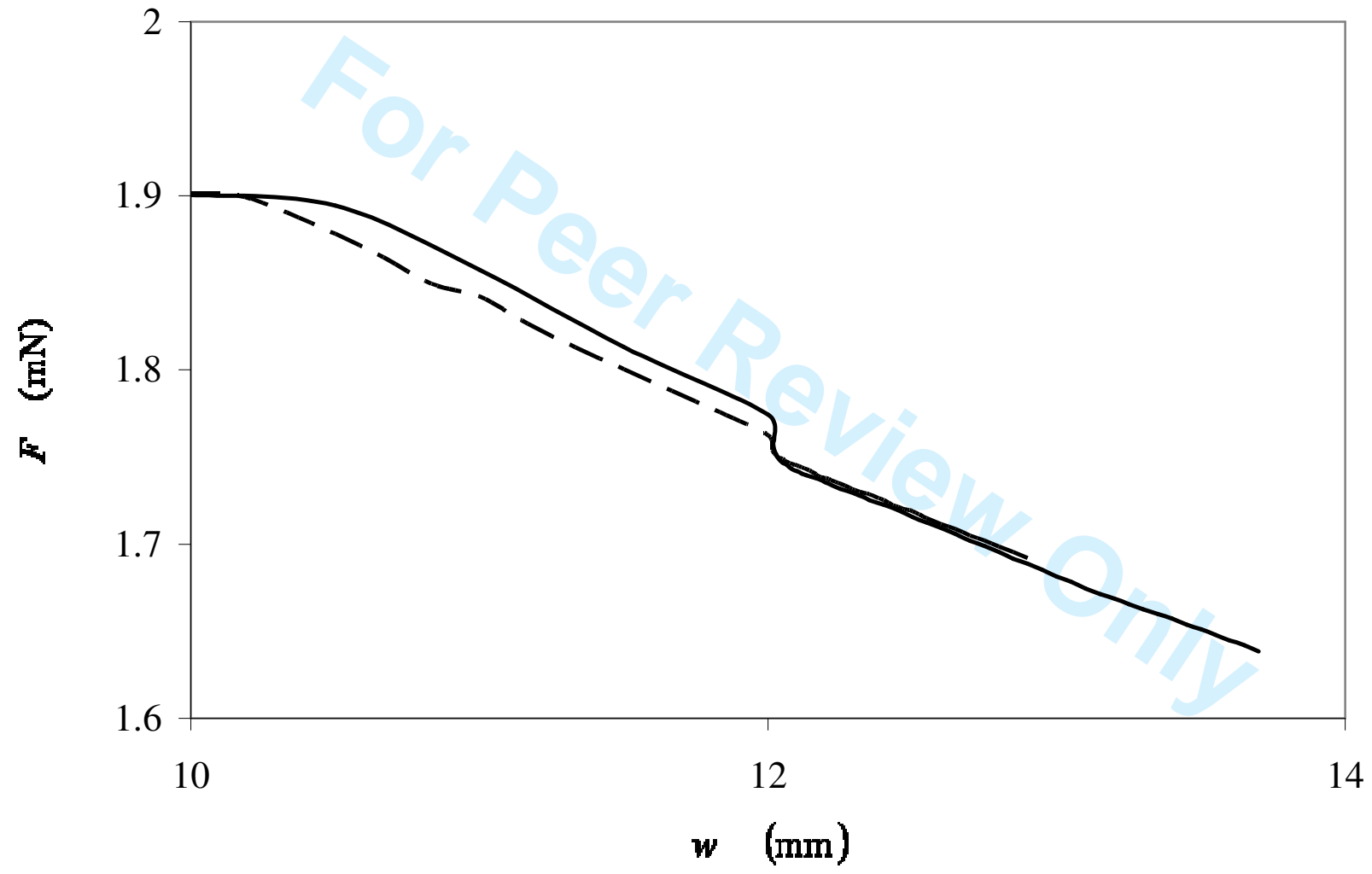
1
2
3
4
5
6
7
8
9
10
11
12
13
14
15
16
17
18
19
20
21
22
23
24
25
26
27
28
29
30
31
32
33
34
35
36
37
38
39
40
41
42
43
44
45
46
47

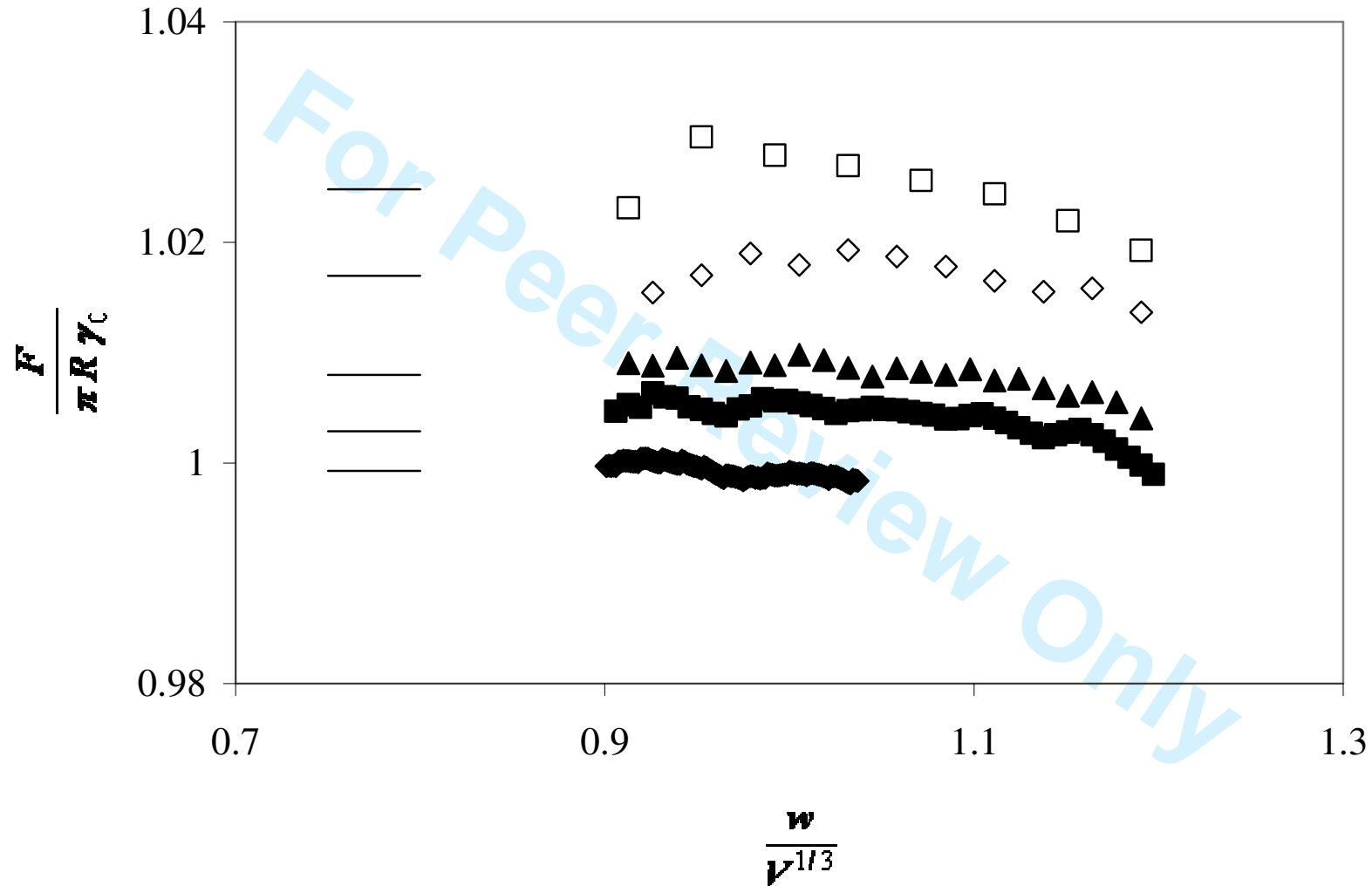
1
2
3
4
5
6
7
8
9
10
11
12
13
14
15
16
17
18
19
20
21
22
23
24
25
26
27
28
29
30
31
32
33
34
35
36
37
38
39
40
41
42
43
44
45
46
47





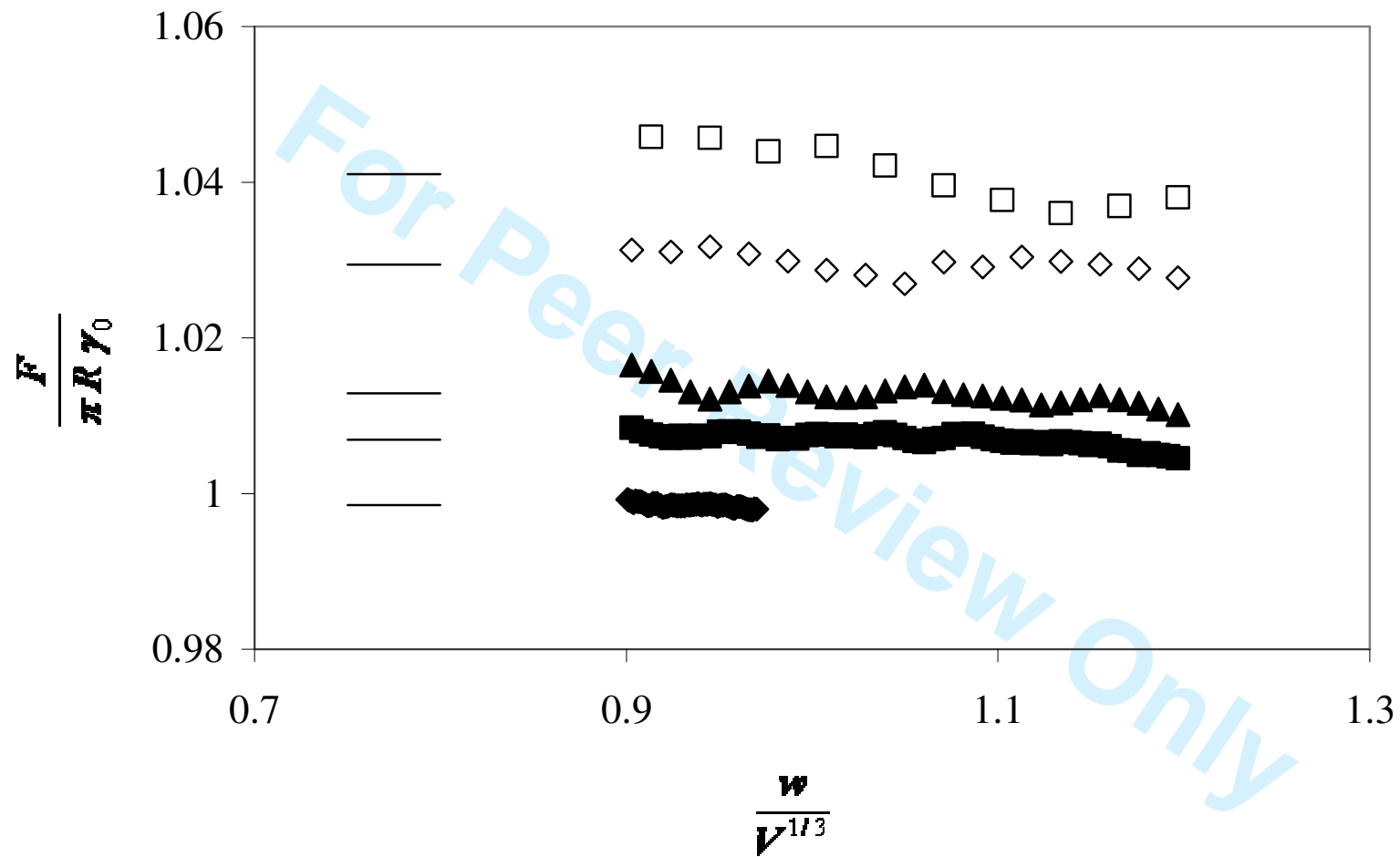
1
2
3
4
5
6
7
8
9
10
11
12
13
14
15
16
17
18
19
20
21
22
23
24
25
26
27
28
29
30
31
32
33
34
35
36
37
38
39
40
41
42
43
44
45
46
47

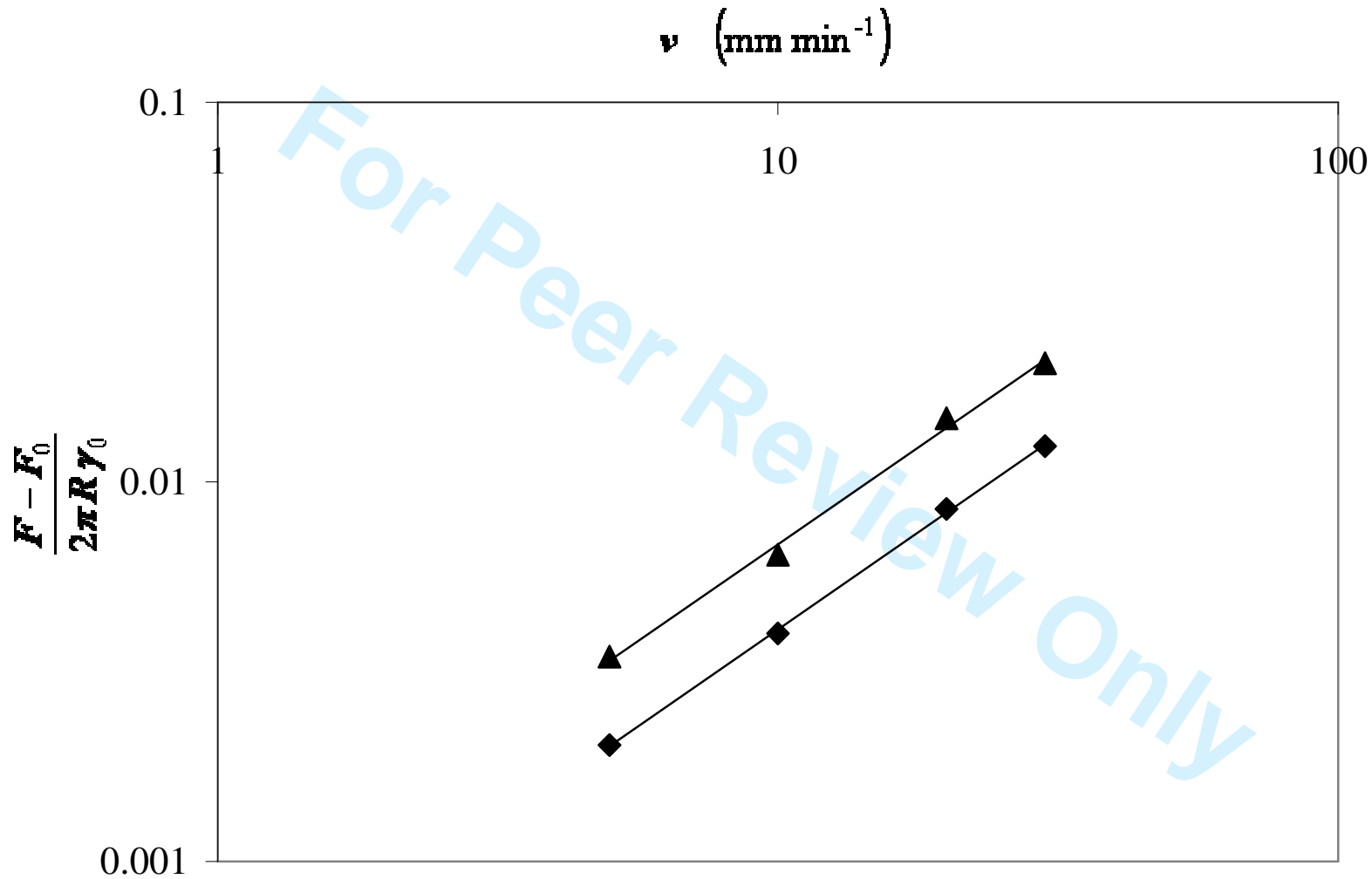




1
2
3
4
5
6
7
8
9
10
11
12
13
14
15
16
17
18
19
20
21
22
23
24
25
26
27
28
29
30
31
32
33
34
35
36
37
38
39
40
41
42
43
44
45
46
47

1
2
3
4
5
6
7
8
9
10
11
12
13
14
15
16
17
18
19
20
21
22
23
24
25
26
27
28
29
30
31
32
33
34
35
36
37
38
39
40
41
42
43
44
45
46
47





1
2
3
4
5
6
7
8
9
10
11
12
13
14
15
16
17
18
19
20
21
22
23
24
25
26
27
28
29
30
31
32
33
34
35
36
37
38
39
40
41
42
43
44
45
46
47

1
2
3
4
5
6
7
8
9
10
11
12
13
14
15
16
17
18
19
20
21
22
23
24
25
26
27
28
29
30
31
32
33
34
35
36
37
38
39
40
41
42
43
44
45
46
47

